Datapages/Search and Discovery Article #90211 CSPG© 2015 CSPG/CSEG/CWLS Convention 2006, What's New? Where is Our Industry Heading? Calgary, AB, Canada, May 15-18, 2006

Seismic Imaging of Imbricate Structures in Mountainous Area: Case Studies

Nanxun Dai[1], Oz Yilmaz[1], Weizhong Wang[1], and Jie Zhang[1]

[1]GeoTomo, Houston, Texas, United States (Ndail@geotomo.com)

Abstract

The hydrocarbon prospects in mountainous areas require solving a most challenging problem in seismic imaging --- irregular topography associated with a rugged terrain, complexity of the near surface that includes high-velocity layers and outcrops with significant lateral velocity variations, complexity of the overburden, and the complexity of the target imbricate structures themselves. We present case studies that demonstrate a workflow to solve this challenging problem: (1) the near surface model is estimated by nonlinear traveltime tomography that accounts for topography, and resolves lateral and vertical velocity variations. (2) Several different strategies are developed for near surface corrections, which are based on wavefield extrapolation rather than shot-receiver statics. (3) The velocity model for prestack time migration is built based on migrated images combined with powerful interactive tools to pick rms velocities that are structurally consistent and the substratum model is estimated by half-space velocity analysis. (4) The subsurface image is obtained by wave equation based prestack depth migration of shot gathers from topography. Theoretical examples and real data cases will be exhibited to demonstrate the methodology.

Introduction

Conventional data analysis in midpoint-offset coordinates often fails to image complex imbricate structures associated with overthrust tectonics. Irregular topography associated with a rugged terrain and complexity of the near surface that includes high-velocity layers and outcrops with significant lateral velocity variations prohibits analytic or linear inversion methods to delineate the near-surface model. Additionally, the nonhyperbolic moveout behavior associated with complex structures and the breakdown of the hyperbolic moveout assumption valid only for small spread lengths prohibit the application of conventional processing in midpoint-offset coordinates to image the subsurface. The analysis workflow presented here, on the other hand, is designed to perform earth modeling and imaging in depth of seismic data in shot-receiver domain from topography.

Near-Surface Modeling

Starting with the field records, we pick first-arrival times, and check the reciprocal errors and make sure that they are sufficiently small. In general, the maximum reciprocal error should be less than 15 ms, and the average of the reciprocal errors for all shots should be less than 10 ms. In theory, reciprocity principal states that interchanging of the shot and receiver locations does not alter the traveltime. However, in practice, errors in geometry, charge depth, mispicks, and heterogeneities near the shot and receiver locations can cause a difference. Large reciprocal errors are often caused by geometry and picking errors. Therefore, the reciprocal error display is used to quality control the geometry and traveltime picks. Next, we bundle the traveltime trajectories to form a general trend that can be associated with laterally invariant but vertically varying velocities within the near surface. We then determine the near-surface layer velocities and thicknesses inferred by the traveltime trajectory and build an initial model for the near surface. We compute the traveltimes associated with all shot and receiver locations by ray tracing using the initial velocity depth model. Then, we perturb the initial model parameters until the difference between the modeled and the observed (actual) traveltimes is minimum in the least-squares sense using nonlinear traveltime tomography (Zhang and Toksoz, 1998) that accounts for the change in traveltime gradient. We iterate until the difference between the modeled and the actual traveltimes, measured as the rms error in inversion, has been reduced to a sufficiently small value comparable to the reciprocal errors. The resulting near-surface model is shown in Figure 1. For quality control, we examine the raypaths associated with the near-surface model and make sure that they do not hit the bottom of the model. This is an indispensable quality control to judge as to the acceptance of the near-surface model. In addition, we examine the differences between the modeled traveltimes associated with the tomography solution for the near surface and the observed (picked) traveltimes, and make sure that the match between the modeled and the observed traveltimes is satisfactory. Finally, from the near-surface model, we pick a floating datum and an intermediate datum that represents the boundary between the near surface and the subsurface regions.

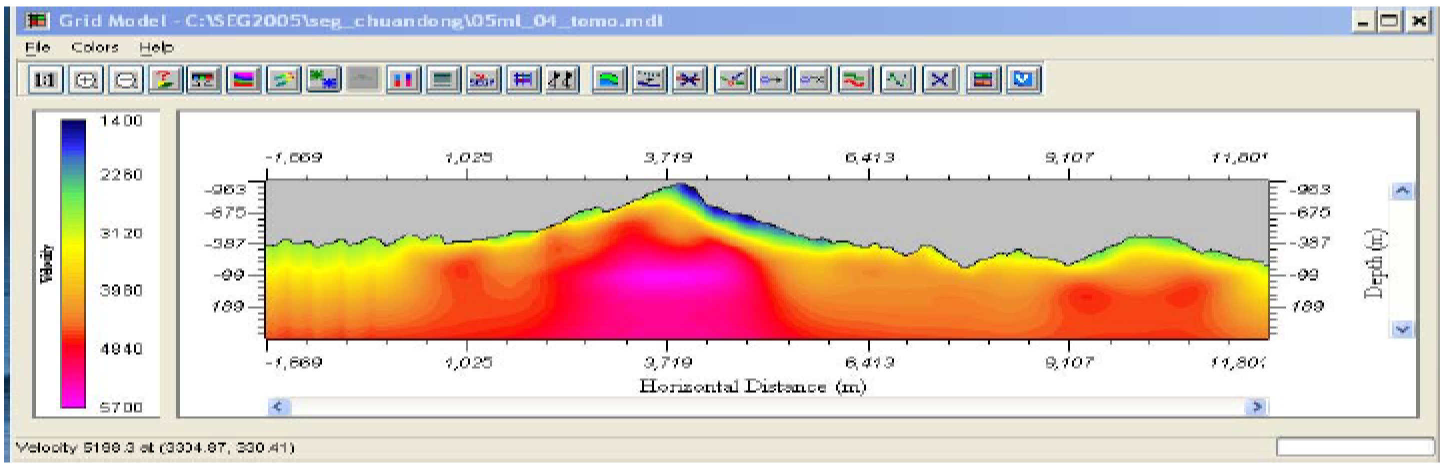

Figure 1. The near-surface model estimated by nonlinear inversion of the traveltimes associated with the first arrivals on shot.

Wavefield Datuming for Near-Surface Corrections

We apply near-surface corrections by wavefield datuming in lieu of shot-receiver statics using the near-surface model. Strategies for near-surface corrections based on wavefield datuming are: (1) statics corrections to replace the near-surface region with the replacement velocity followed by wave extrapolation from topography up to the seismic reference datum above the topography by using the replacement velocity; (2) wave extrapolation from topography down to a flat datum below the intermediate datum using the near-surface velocity-depth model; and (3) wave extrapolation from topography down to the intermediate datum using the near-surface velocity field followed by wave extrapolation up to the seismic reference datum using the replacement velocity.

Subsurface Modeling and Imaging in Depth

Following the application of an appropriate near-surface strategy, we perform prestack time migration of shot gathers using a range of constant velocities and create an rms velocity cube (Shurtleff, 1984). We then interpret this image volume to derive an rms velocity field associated with events in their migrated positions (Yilmaz, 2001). This rms velocity field is better suited for Dix conversion to derive an interval velocity field compared to Dix conversion of stacking or DMO velocities, which are associated with events in their unmigrated positions. We use the three cross sections of the velocity cube for picking the rms velocities (Figure 2). These are the distance along the line traverse versus event time after migration for a given rms velocity --- the X-T plane, the rms velocity versus event time after migration for a specific location along the line traverse--- the V-T plane, and the rms velocity versus the distance along the line traverse for a specific time --- the V-X plane that represents a time slice from the velocity cube. We scan the X-T planes and pick horizon strands associated with the best image with the highest amplitude.

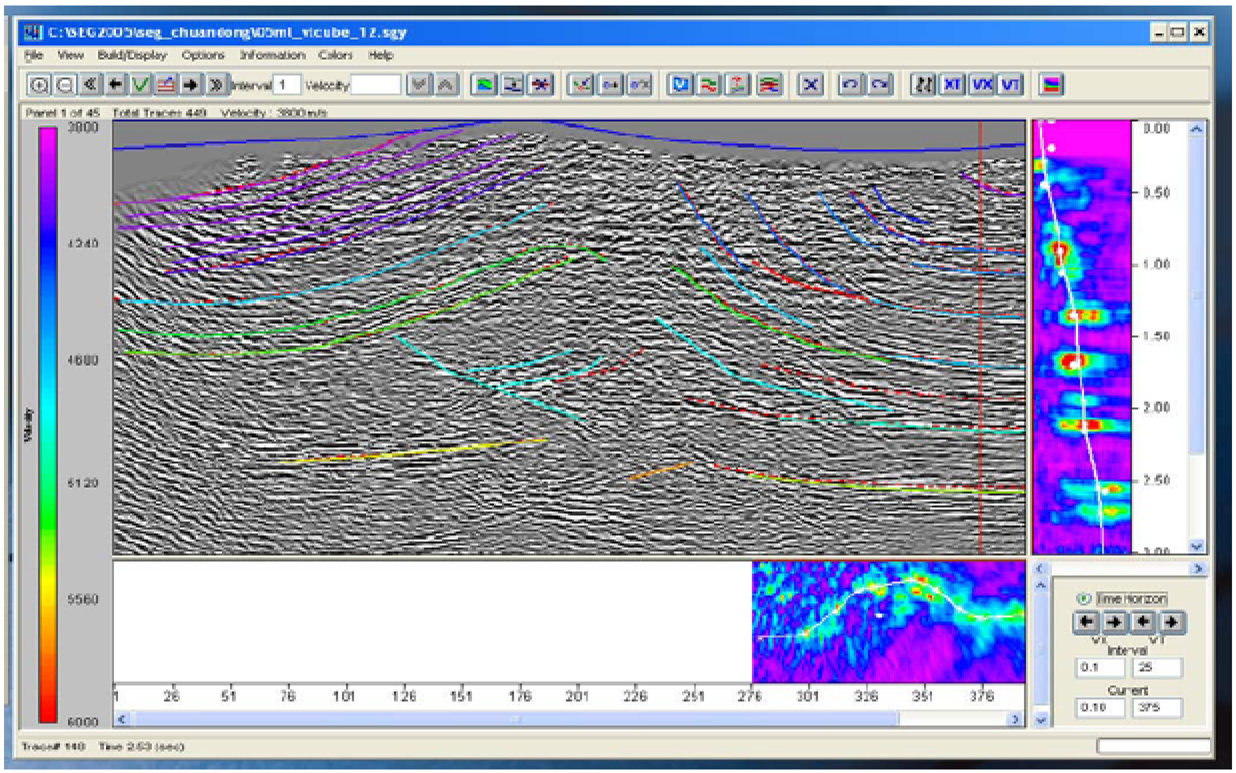

Figure 2. The X-T (top), V-T (right), and V-X (bottom) cross-sections of the rms velocity-cube. The image panels in the X-T lane are used to pick horizon strands and the semblance spectra in the V-X plane are used to pick velocity strands, while the semblance spectrum in the V-T plane is used to quality control the picks.

We then pick the velocity strand associated with the horizon strand from the semblance spectrum in the V-T plane. We use the semblance spectrum in the V-T plane for quality control of the picked velocity strands. While the X-T plane provides structural consistency, the V-X plane provides the lateral consistency in picking the velocity strands. We combine all the velocity strands and create an rms velocity field associated with events in their migrated positions. We migrate the shot gathers using the rms velocity field derived from the interpretation of the velocity cube based on the selected near-surface strategy. We then unmigrate (demigrate) the resulting image from prestack time migration using the same rms velocity field as for prestack time migration. The demigrated section is a representation of a zero-offset wavefield; as such, it is the appropriate input to poststack depth migration compared to the conventional stack, which is only an approximate representation of a zero-offset section.

Strategies to estimate the velocity-depth model for the subsurface are: (1) Dix conversion of rms velocities; and (2) layer-by-layer half-space velocity analysis. In case of strategy 1, we perform poststack depth migration of the demigrated section from using the interval velocity field. To estimate the velocity-depth model for the subsurface region where depth migration is imperative, we perform strategy 2 based on layer-by-layer half-space velocity analysis (Yilmaz, 2001). Given the overburden model already estimated, we assign a set of constant velocities to the underlying half-space that include the layers yet to be resolved. We perform prestack depth migration and obtain a set of images that we use to pick the velocity that best images the base of the layer under consideration. We repeat this process for as many layers as needed. Finally, we perform depth migration of the shot gathers of from topography, individually, and sort the shot images to common-reflector gathers (CRP) in depth (one type of image gathers), and stack the CRP gathers to obtain the image in depth (Figure 3).

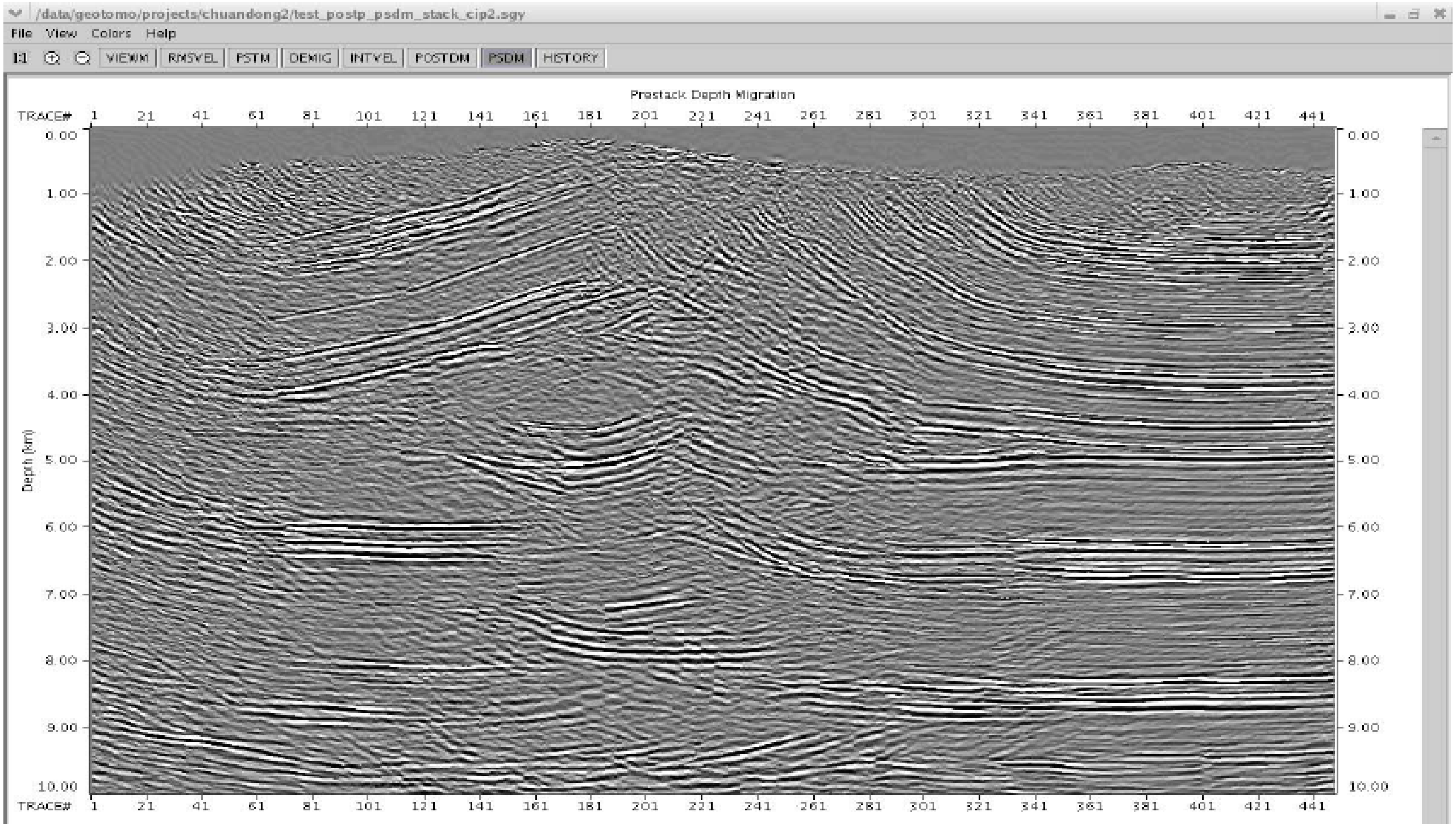

Figure 3. Image from prestack depth migration using velocity-depth model based on layer-by-layer half-space velocity analysis.

Conclusions

We have applied an earth modeling strategy to image complex structures in the Southwest China Thrust Belt. The workflow involves: (1) near-surface modeling by the application of nonlinear traveltime tomography to the first arrival times picked from field records; (2) near-surface corrections by wavefield datuming, and (3) subsurface modeling by half-space velocity analysis and prestack depth migration of shot gathers from topography.

Acknowledgements

We thank Sichuan Geophysical Company for providing the seismic data used in this case study and granting us the permission to publish the results.

References Cited

Shurtleff, R., 1984, An F-K procedure for prestack migration and velocity analysis: Presented at the 46th Ann. Mtg. European Asn. Expl. Geophys.

Yilmaz, O., 2001, Seismic Data Analysis: Society of Exploration Geophysicists, Tulsa.

Zhang, J. and M.N. Toksoz, 1998, Nonlinear refraction traveltime tomography: Geophysics, v. 63, p. 1726-1737.